MolecularMedicine

Peptide Mimetic of the S100A4 Protein Modulates Peripheral Nerve Regeneration and Attenuates the Progression of Neuropathy in Myelin Protein P_0 Null Mice

Mihai Moldovan,[1] Volodymyr Pinchenko[1,2*] Oksana Dmytriyeva,[2*] Stanislava Pankratova,[2] Kåre Fugleholm,[3] Jorg Klingelhofer,[2] Elisabeth Bock,[2] Vladimir Berezin,[2] Christian Krarup,[1,4] and Darya Kiryushko[2]*

[1]Nerve Laboratory, Department of Neuroscience and Pharmacology, Panum Institute, University of Copenhagen, Copenhagen, Denmark; [2]Protein Laboratory, Department of Neuroscience and Pharmacology, University of Copenhagen, Copenhagen, Denmark; [3]Department of Neurosurgery, Rigshospitalet, Copenhagen, Copenhagen, Denmark; and [4]Department of Clinical Neurophysiology, Rigshospitalet, Copenhagen, Denmark

We recently found that S100A4, a member of the multifunctional S100 protein family, protects neurons in the injured brain and identified two sequence motifs in S100A4 mediating its neurotrophic effect. Synthetic peptides encompassing these motifs stimulated neuritogenesis and survival *in vitro* and mimicked the S100A4-induced neuroprotection in brain trauma. Here, we investigated a possible function of S100A4 and its mimetics in the pathologies of the peripheral nervous system (PNS). We found that S100A4 was expressed in the injured PNS and that its peptide mimetic (H3) affected the regeneration and survival of myelinated axons. H3 accelerated electrophysiological, behavioral and morphological recovery after sciatic nerve crush while transiently delaying regeneration after sciatic nerve transection and repair. On the basis of the finding that both S100A4 and H3 increased neurite branching *in vitro*, these effects were attributed to the modulatory effect of H3 on initial axonal sprouting. In contrast to the modest effect of H3 on the time course of regeneration, H3 had a long-term neuroprotective effect in the myelin protein P_0 null mice, a model of dysmyelinating neuropathy (Charcot-Marie-Tooth type 1 disease), where the peptide attenuated the deterioration of nerve conduction, demyelination and axonal loss. From these results, S100A4 mimetics emerge as a possible means to enhance axonal sprouting and survival, especially in the context of demyelinating neuropathies with secondary axonal loss, such as Charcot-Marie-Tooth type 1 disease. Moreover, our data suggest that S100A4 is a neuroprotectant in PNS and that other S100 proteins, sharing high homology in the H3 motif, may have important functions in PNS pathologies.

Online address: http://www.molmed.org
doi: 10.2119/molmed.2012.00248

INTRODUCTION

The multifunctional S100 protein family plays an important role in many human diseases and governs processes such as apoptosis, inflammation and cell motility (1–3). Several S100 proteins are overexpressed in the nervous system during neurodegeneration and neuronal plasticity (4–6). Specifically, one member of the S100 protein family called the S100A4 (Mts1) is upregulated at sites of lesion in the brain. However, being initially identified as a metastasis promoter, S100A4 was mainly studied in relation to cancer (reviewed in [7,8]), and its function in the injured nervous system remains unclear.

In the lesioned brain, S100A4 is upregulated in the white matter astrocytes outlining the trauma site (9) and is also detected in the hippocampus after excitotoxic injury (10). S100A4 is also overexpressed by the astrocytes of the spinal cord adjacent to the site of spinal transection (11). *In vitro* studies have shown that S100A4 can be secreted by several cell types including astrocytes (10,12,13) and exert extracellular effects, such as promoting neurite outgrowth and survival of primary hippocampal and cerebellar neurons (10,14–16). These findings suggest that S100A4 may, in addition to its conventional role in carcinogenesis, also modulate posttraumatic events in the nervous system. Supporting this hypothesis, we recently found that S100A4 knockout increases neuronal loss after traumatic brain injury and identified two neurotrophic motifs in the S100A4 sequence (10). Synthetic peptides corresponding to these motifs (H3 and H6)

**MM, VP, and OD contributed equally to this work.*

Address correspondence to *Christian Krarup, Department of Clinical Neurophysiology, Rigshospitalet, Blegdamsvej 9, 2100 Copenhagen, Denmark. Phone: +45-35-45-30-60; Fax: +45-35-45-32-64; E-mail: christian.krarup@regionh.dk.*

Submitted June 12, 2012; Accepted for publication March 7, 2013; Epub (www.molmed.org) ahead of print March 8, 2013.

The Feinstein Institute for Medical Research North Shore LIJ

stimulated neuritogenesis and survival of cultured neurons and, most importantly, mimicked the S100A4-induced neuroprotection *in vivo*. Altogether, these findings suggest that S100A4 protects neurons in the injured central nervous system (CNS) via neuritogenic and prosurvival effects and possibly contributes to glial–axonal interactions.

Although S100A4 has been less investigated in the peripheral nervous system (PNS) than in the CNS, several studies indicate that its expression also increases in myelinating Schwann cells and/or unmyelinating Remak bundles at the injury site after dorsal root or peripheral nerve injury (17,18). Increased S100A4 levels after injury were also found in a subpopulation of neurons, mainly sensory and autonomic (18). Moreover, S100A4 promoted neurite outgrowth from sensory neurons *in vitro* (19), and the S100B member of the family was shown to stimulate neurite outgrowth in the rat sciatic nerve (20). Here we hypothesize that, similar to the CNS, S100A4 exerts proregenerative and/or prosurvival effects in the injured PNS. Specifically, the aim of this study was to investigate the effect of S100A4 mimetics in the *in vivo* rodent PNS lesion models, with an emphasis on the regeneration and survival of myelinated axons. Peripheral nerves were evaluated by combining nerve conduction, behavioral and histological studies, reflecting different aspects of peripheral nerve recovery (21).

To investigate the proregenerative effects of S100A4 mimetics, we used two nerve lesion models, on the basis of crush or transection and reconstruction (see Wolthers *et al.* [21] for details). Nerve crush leaves endoneurial tubes intact, allowing an accurate target-organ reinnervation, whereas nerve transection (the common clinical lesion type) disrupts endoneurial tubes, thereby causing axonal misdirection. The use of these models allows separating effects related to axonal growth from those related to axonal branching and path-finding.

To study the prosurvival effects of S100A4 mimetics, we used mice deficient in the myelin protein zero (P_0) gene, a well-established model of dysmyelinating Charcot-Marie-Tooth type 1 (CMT1) inherited human neuropathy. P_0 knockout mice show a severe progressive loss of myelin and degeneration of both motor and sensory myelinated axons (22,23). Although the precise mechanism of axonal degeneration in CMT1 is unknown, several lines of evidence point toward an altered axon–Schwann cell interaction (24,25), which makes this model particularly suitable to investigate the effects of S100A4.

By using these approaches, we found that the H3 peptide mimetic of S100A4 affects the time course of peripheral nerve regeneration and has important axonal prosurvival effects in P_0 null mutants.

MATERIALS AND METHODS

Animals and Experimental Design

In a first series of experiments, the effect of the H3 and H6 peptides on sciatic nerve regeneration after crush was investigated in Wistar rats (Taconic, Lille Skensved, Denmark) treated daily (subcutaneous [s.c.] injections for 3 wks) with vehicle (n = 10), H3 (10 mg/kg, n = 10) and H6 (10 mg/kg, n = 10). During the study, regeneration was followed by serial functional tests (walking-track analysis and pinprick). At the completion of the study, intact and injured sciatic nerves and plantar skins were harvested for histological analysis. The *in vitro* effects of H3 were investigated in cultured rat hippocampal and motor neurons isolated as described below.

In a second series of experiments, the effect of H3 on sciatic nerve regeneration was investigated in C57BL/6J mice (Taconic) after transection (n = 14) and crush (n = 22). The mice were randomly distributed in vehicle- and H3-treated groups (10 mg/kg s.c., alternate day injections). The treatment was continued for 4 wks from the time of the lesion, followed by a further observation period of 2 wks after crush or 5 wks after section. During the study, the recovery was monitored by serial nerve conduction studies and a functional test (walking track analysis). At the completion of the studies, intact and injured tibial nerves were harvested for histological evaluation.

In a third series of experiments, the effect of H3 on neuropathic axonal loss was investigated in 2-month-old myelin protein P_0 gene null mice of C57BL background (n = 16), hereafter called $P_0^{-/-}$ (22). Heterozygous P_0 mice were bred at Copenhagen University (Denmark). DNA was extracted from tail clips (Qiagen DNeasy Blood & Tissue Kit; Qiagen, Copenhagen, Denmark). $P_0^{-/-}$ offspring were identified by a conventional polymerase chain reaction with the primers 5′-TCAGTTCCTTGTCCCCCGCTCTC-3′, 5′-GGCTGCAGGGTCGCTCGGTGTTC-3′ and 5′-ACTTGTCTCTTCTGGGTAAT CAA-3′ (Sigma-Aldrich, Brøndby, Denmark), generating amplicons of 334 or 500 bp for the P_0 null mutation and wild-type alleles, respectively (26). The mice were randomly distributed in vehicle- and H3-treated groups (10 mg/kg s.c., alternate day injections). The treatment was performed for 4 wks. Before and after the treatment, the mice were evaluated by nerve conduction tests and a functional test (rotarod). At the completion of the experiments, all tibial nerves were harvested for histological evaluation. In all studies, the investigators were blinded to the treatment.

For surgical procedures and electrophysiological investigations, mice were anesthetized with a mixture of fentanyl/droperidol/midazolam (0.45/30/3 mg/kg). Surgical procedures in rats were also carried out under a mixture of fentanyl/droperidol/midazolam (0.002/0.14/0.014% w/v, s.c.).

At the completion of the experiments, the animals were killed by a lethal dose of pentobarbital or cervical dislocation (mice). Animal care was conducted in accordance with the *OECD Principles on Good Laboratory Practice* (27). All experiments were performed according to European Union (EU) legislation (Directive 2010/63/EU [28]) and international

guidelines (29), with a license from the Danish Animal Experiment Inspectorate.

Peptide Mimetics of S100A4

The H3 (KELLTRELPSFLGKRT) and H6 (NEFFEGFPDKQPRKK) peptides were synthesized as tetramers composed of four monomers coupled to a lysine backbone via the α- and ε-amino groups (Schafer-N ApS, Copenhagen, Denmark). Tetramerization was previously found to be necessary for the neuritogenic activity of S100A4 (14).

Nerve Lesions

Sciatic nerve crush in rats. A longitudinal cutaneous incision was made on the back of the thigh. The sciatic nerve was exposed over a length of 2–2.5 cm and unilaterally crushed twice in the same place (0.5 cm proximal to sciatic nerve trifurcation) for 30 s by using a locking surgical needle holder. The wound was closed with 5-0 suture material, and the rats were allowed to recover. The contralateral (unoperated) side served as a control.

Sciatic nerve lesion in mice. Surgical procedures were performed under a stereomicroscope (MZ6; Leica Microsystems, Wetzlar, Germany). The right sciatic nerve was lesioned through a minimal incision at the mid-thigh level (~1 cm above the knee). The sectioned nerves were immediately repaired with two to three interrupted epineurial 10-0 sutures. Crush lesions were performed by maximally clamping the nerve with a smooth-jawed microforceps for 30 s. The wounds were closed with three sutures (5-0), and mice were allowed to recover. After crush in both mice and rats, the injured nerve remained translucent and in continuity. No animal weight loss was observed during the study.

Electrophysiological Investigations of the Mouse Tibial Nerve

The anesthetized mouse was fixed in a stereotaxic frame (dual manipulator with mouse adaptor 51624; Stoelting, Wood Dale, IL, USA) on a temperature-controlled pad set to 37°C (HB 101/2; LSI Letica, Barcelona, Spain). The investigated leg was placed on a piece of hydrophobic cotton and clamped at the distal toes as previously described (30).

Electrical stimuli with a duration of 0.2 ms were delivered by a constant current stimulator (A395 linear stimulus isolator; WPI, Sarasota, FL, USA) to the tibial nerve via custom-made platinum needle electrodes. The cathode was inserted at the ankle, and the anode was inserted ~0.5 cm proximally. The evoked compound muscle action potential (CMAP) was recorded (10 Hz to 6 kHz; 10C02, Dantec, Copenhagen, Denmark) from plantar muscles using needle electrodes inserted into the foot ~0.5 cm apart: the active electrode was placed medially at the base of the foot and the reference distally at the second toe. A ground electrode was inserted subcutaneously between the stimulation and recording electrodes.

The needles caused negligible damage to the muscles or the near nerve tissue, so that reproducible CMAP recordings could be obtained with repeated daily testing in this model (30). CMAP amplitudes were measured peak to peak. Latencies were measured to the first deflection from baseline, evaluating the conduction of the fastest motor axon.

Functional Tests

Walking track in rats and mice. In rats, functional recovery was assessed every 2 d after surgery by walking-track analysis (21). Each rat walked one to three times per test to obtain the best possible representative tracks. Several prints of each foot were inspected, and the best corresponding pair of prints from the experimental (E) and normal (N) legs was measured to the nearest millimeter, by using a caliper. Three footprint parameters were measured: the distance from heel to the third toe—print length (PL); the distance between the first and fifth toes—toe spread (TS); and the distance between the second and fourth toes—the intermediary toe spread (IT).

The sciatic functional index (SFI) (31,32) was determined as follows: SFI = –38.3 [(EPL – NPL)/NPL] + 109.5 [(ETS – NTS)/NTS] + 13.3 [(EIT-NIT)/NIT] – 8.8. The calculated SFI varied between 0 (for uninjured) and approximately –100 (for maximally impaired gait).

In mice, the SFI estimation using footprints on paper is not readily feasible. Instead, we used a custom-made glass stage with lateral illumination in a dark room so that only the reflected light at the contact points with the paws was recorded by a high-resolution video camera placed below the stage. Thereafter, still frames from the video were extracted and the PL, TS and IT of 7–10 footprints per mouse were quantified by using the measuring tool in PhotoShop CS2 (Adobe, San Jose, CA, USA), averaged and used for SFI determination.

Pinprick test in rats. The recovery of pain sensitivity was tested in awake animals by lightly pricking the plantar heel area with a needle. The test was performed 2 d before surgery to obtain the baseline and then twice per week for up to 3 wks after surgery. A pinprick score was assigned from no response (0), reduced or inconsistent responses (1), to normal reaction (2). The normal response was withdrawal of the paw and /or vocalization.

Rotarod in mice. Motor performance was evaluated by using an Ugo Basile 7650 accelerating rotarod (Ugo Basile, Comerio, VA, Italy). After the mice were placed on the rod, the counter was started and the rod was accelerated from 4 to 40 rpm over a 300-s period. Any mouse remaining on the apparatus after 600 s was removed, and the time was scored as 600 s. Each determination represents the longest endurance time of three consecutive measurements repeated at ~10-min intervals.

Histology

Immunohistology of sciatic nerve (S100) and plantar skins (PGP 9.5). The plantar skin of the hind paws and 5-mm-long fragments of regenerated sciatic nerves 5 mm distal to the crush site were removed, fixed in Zamboni solution at 4°C overnight and equilibrated in 30%

buffered sucrose (pH 7.4). Cryosections (30 μm for sciatic nerve and 80 μm for plantar skins) were washed free-floating in 0.01% Nonidet P-40/Tris-buffered saline (TBS). Endogenous peroxidase activity was eliminated by 15-min incubation in 1.5% H_2O_2 in TBS, and nonspecific binding was blocked with 10% goat serum (In Vitro, Fredensborg, Denmark) in TBS-Nonidet (1 h at room temperature). The samples were then incubated overnight at 4°C with rabbit anti-human S100 (1:500; DakoCytomation, Glostrup, Denmark; sciatic nerve sections), or mouse anti-human protein gene product 9.5 clone 31A3 (PGP 9.5) (1:800; Biogenesis, Kidlington, UK; plantar skin sections). The anti-S100 primary antibodies were detected by using biotinylated anti-rabbit IgG (1:400; Sigma-Aldrich) enhanced by StreptABComplex–HRP (DakoCytomation) as described by the manufacturer. Immunostainings were visualized by using 0.015% (v/v) H_2O_2 in 3,3′-diaminobenzidine. Anti-PGP 9.5 primary antibodies were detected with the Alexa Fluor 488 goat anti-mouse IgG (Invitrogen; Life Technologies, Carlsbad, CA, USA).

Osmium staining and S100A4 immunostaining of tibial nerve sections in mice. The tibial nerves were removed and fixed by immersion in glutaraldehyde (2.0% in 0.1 mol/L cacodylate buffer) for 24 h. The fixed nerves were postfixed in 1% osmium tetroxide in 0.1 mol/L Sørensen buffer, dehydrated in graded alcohol (30–100%), cleared in propylene oxide and embedded in increasing concentrations of epoxy resin until polymerized in pure Epon in a heated cabinet. Cross-sections of the tibial nerve at the ankle (corresponding to the electrophysiological stimulation site) were cut with dry glass knives at 2–3 μm, overstained with p-phenylenediamine and mounted for light microscopy.

For S100A4 immunostaining, controlled surface corrosion of the Epon-embedded sections was performed by etching the section for 45 min in a 50% solution of saturated sodium hydroxide in absolute ethanol, followed by rehydration with descending concentrations of ethanol. Thereafter, the sections were processed and stained by using the above-described protocol for S100 immunostaining and rabbit anti-mouse S100A4 antibodies (1:2,000; characterized by Dmytriyeva *et al.* [10]).

Microscopy and morphometric analysis. Images were acquired by using an Olympus BX-51 microscope (Olympus Danmark, Ballerup, Denmark), with the 40 × 1.4, 60 × 1.4 or 100 × 1.4 objective, and the Visiopharm Integrator System (33) software (Visiopharm, Hoersholm, Denmark). In rats, the number of S100-positive fibers was quantified from the S100-stained cross-sections of the tibial nerve 5 mm distal to the nerve crush level. Micrographs of the rat nerves to be analyzed were randomly captured in nonoverlapping areas covering 20–25% of the total cross-sectional area of the nerve. The axon and fiber diameters were measured in 300–500 fibers of each nerve. To evaluate the area of PGP 9.5 immunoreactivity in rats, three sections of plantar skin from each hind paw were chosen, and 8–10 images were collected from each section. The total image area and positive reactivity area were measured by using PrAverB image analysis software (Protein Laboratory, University of Copenhagen, Copenhagen, Denmark). The percentage of positive reactivity was calculated as Ap/Af × 100, where Ap is the total area of positive reactivity, and Af is the total area of the field.

Nerve morphometry in mice was performed on osmium-stained tibial nerves at the ankle (the electrophysiological stimulation site), at least 1 cm distal to the injury site. Precise distance measurements were not carried out because the distal end of the investigated segment was clearly defined by anatomical landmarks in mice of a similar age. As controls, images of uninjured nerves were taken at the corresponding level. For axonal quantification of mouse nerves, images were processed by using the custom-made MNERVE morphometry software developed in MATLAB (version 2010a; MathWorks, Natick, MA, USA). First, the total endoneurial area was traced from the overview micrographs. Detailed micrographs (at least 10% of the total nerve area) were then used to trace the myelin rings. The axonal and fiber diameters were calculated as the diameters of the circle having the same area as the inner and outer contours of the myelin rings, respectively. Incomplete myelin rings (that is, at the border of the measured region) were not counted. The total number of myelinated axons was calculated as the total endoneurial area multiplied by the fiber density within the measured area.

Neurite Outgrowth Assay

Rat hippocampal neurons (E19) were isolated as previously described (34) and plated at a density of 5,000 cells per well in eight-well LabTek Permanox slides (NUNC, Roskilde, Denmark) coated with laminin (5 μg/mL; Sigma-Aldrich). The cells were stimulated with the peptide or S100A4 and grown for 24 h. To evaluate neurite outgrowth, the cultures were stained with polyclonal rabbit anti-rat growth-associated protein-43 antibodies and analyzed by using computer-assisted microscopy as described previously (34).

For isolation of motoneurons, the ventral horns of the lumbar spinal cord were dissected from Wistar rat embryos (E15) in Ca^{2+}- and Mg^{2+}-free Hanks balanced salt solution supplemented with 40 U/mL penicillin, 40 μg/mL streptomycin, 10 mmol/L HEPES, 1 mmol/L sodium pyruvate (all Gibco; Life Technologies) and 30 mmol/L glucose (Sigma-Aldrich). The cells were trypsinized as described above for hippocampal culture, plated at a density of 7,000 cells per well in eight-well LabTek Permanox slides (NUNC) coated with laminin (1–5 μg/mL) and stimulated with H3 or S100A4 for 24 h. To confirm cell identity, the cultures were stained with monoclonal mouse antibodies against neurofilament-HT known to be specific for motoneurons in dissociated spinal cord cultures (35). To evaluate neurite outgrowth, the cultures were stained with polyclonal rabbit anti-rat

growth-associated protein 43 (GAP-43) antibodies and analyzed as described by Pankratova *et al.* (36).

Statistics

Statistics and graphical presentations were performed by using Origin 6.1 software (OriginLab, Northampton, NY, USA) and GraphPad Prism 4.0 for Windows (GraphPad, San Diego, CA, USA). Statistical comparisons were performed using one-way analysis of variance (ANOVA) or two-tailed *t* test. The Wilcoxon rank-sum test was used to evaluate the pinprick data. The results are given as mean ± standard error of the mean. Unless stated otherwise, asterisks indicate statistical significance: $*p < 0.05$; $**p < 0.01$; $***p < 0.001$.

RESULTS

Peptide Mimetics of S100A4 Accelerated the Recovery after Sciatic Nerve Crush in Rats

We previously found that the S100A4 protein increases neuritogenesis and survival of primary neurons, and this effect is mediated by two motifs in the S100A4 sequence, H3 and H6 (Figure 1A) (10). Because synthetic peptides corresponding to these motifs mimicked biological activities of S100A4 in animal models of brain trauma, we asked whether H3 and H6 also affect PNS regeneration after injury. Rats were subjected to a nerve crush, followed by daily administration of the H3 or H6 peptides for 21 d after operation. Of the 30 rats included in the study, 28 completed the observational period. Consistent with previous studies (21), restoration of a nerve function, reflected by the SFI, followed a sigmoidal curve (Figure 1B). The recovery of the SFI was significantly accelerated by the H3 peptide, reaching the statistical significance by wk 2 (Figure 1B). Nevertheless, in both H3 and vehicle groups, the SFI recovery plateau attained was within 10% of baseline. Hence, the effect of H3 was a ~2-d leftward shift in the SFI recovery sigmoid (Figure 1B). The H6 peptide had no effect on the SFI time course (Figure 1B).

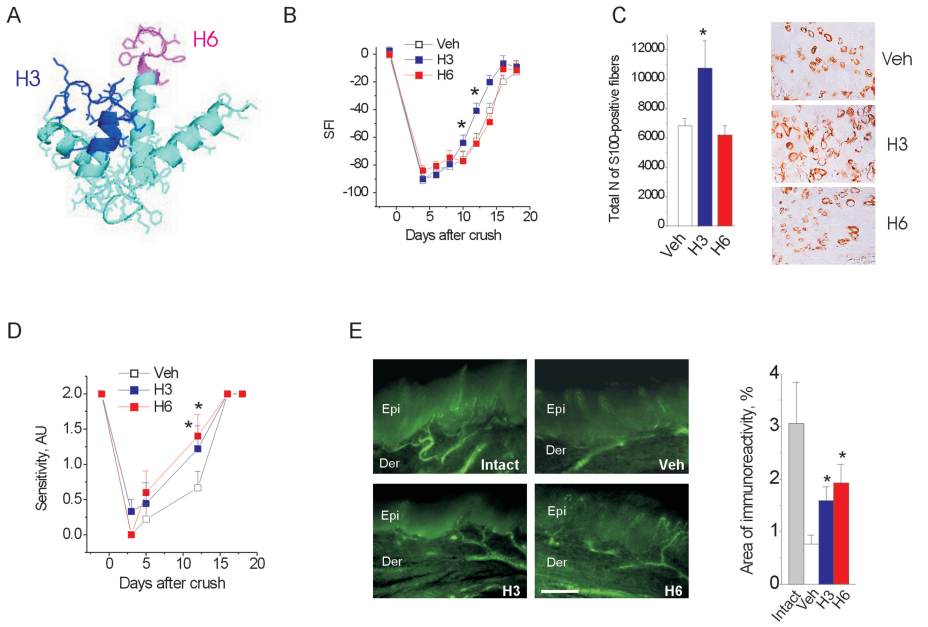

Figure 1. Peptide mimetics of S100A4 affect recovery after sciatic nerve crush in rats. (A) Neuritogenic motifs of S100A4 (H3 and H6) mapped on the three-dimensional structure of the protein (PDB: 1M31). (B, C) H3, but not H6, promotes restoration of an SFI after crush injury (B) and increases the number of S100-positive fibers in the regenerated sciatic nerve at 3 wks after crush (C). $*p < 0.05$ versus vehicle (Veh), one-way ANOVA. (A–E) Veh, H3 and H6 indicate the lesioned side of the vehicle-, H3-, and H6-treated groups, respectively. (D) S100A4 mimetics promote restoration of a sensory function after crush injury, as assessed by the pinprick test. A pinprick score was assigned from no response (0), reduced or inconsistent responses (1), to normal reaction (2). (E) S100A4 mimetics increase sensory reinnervation after crush injury to >50% of intact (unlesioned side of the vehicle-treated group). Left, fluorescent micrographs of regenerated sensory terminals in the plantar paw skin 21 d after crush, anti-PGP 9.5 immunostaining. Scale bar = 100 μm. Epi, epidermis; Der, dermis. Right, quantification of sensory innervation in the epidermis, $*p < 0.05$ versus Veh, one-way ANOVA. (A–E) Number of animals, n = 9/10/10 (Veh/H3/H6).

The S100 proteins are detected in Schwann cells and overexpressed at sites of neural lesions. Moreover, as we have recently found, S100A4 can be upregulated in an autocrine manner (10). The histological evaluation of sciatic nerve sections 3 wks after crush showed that treatment with H3 but not H6 increased the number of S100-positive fibers in regenerated nerves (Figure 1C).

S100A4 mimetics also affected the recovery of sensory function after nerve crush. The sensory response, assessed using the pinprick test, was restored more rapidly in the H3- and H6-treated groups compared with vehicle-treated controls (Figure 1D). To confirm that the observed difference in the functional response was due to the improved sensory reinnervation, we evaluated the density of regenerated sensory fibers in the glabrous skin of the hind paw by using immunostaining for the neuronal marker PGP 9.5. Indeed, 3 wks after nerve crush, the density of the PGP 9.5 immunoreactive fibers in the dermis and epidermis was markedly higher in H3- and H6-treated animals than in vehicle-treated controls (Figure 1E), suggesting an increased sensory and, possibly, sympathetic reinnervation. To summarize, both peptides improved sensory function after crush; however, only H3 accelerated the gait restoration (SFI), although without

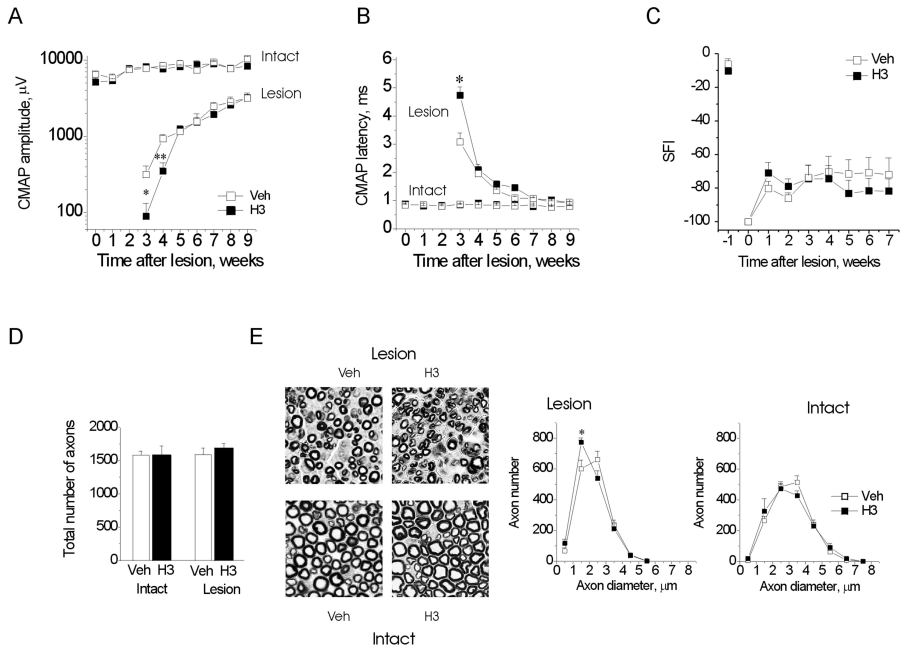

Figure 2. H3 delays axonal regeneration after nerve transection in mice. (A, B) Development of CMAP amplitude (A) and conduction velocity (B) in unoperated (Intact) and operated (Lesion) nerves in the vehicle (Veh)- and H3-treated animals. (C) Recovery of the functional index (SFI). (D, E) Total number of fibers (D) and myelinated fiber distributions (E, right) at 8 wks after lesion. (E, left) Representative images of regenerated sciatic nerves from the vehicle- and H3-treated animals at 8 wks after transection, 50 × 50 μm fields are shown. (A–E) $*p < 0.05$ versus Veh, two-tailed *t* test. (A–C) Number of animals, n = 7/7 (Veh/H3). (D, E) n = 4/4.

changing the functional outcome. On the basis of this finding, we focused our subsequent study on the effects of H3 in the injured PNS.

H3 Delayed the Recovery after Sciatic Nerve Transection but Not after Nerve Crush in Mice

We next tested whether treatment with the H3 peptide affects nerve regeneration after a sciatic nerve transection and repair. The mice subjected to the nerve section and repair were treated with H3 three times a week for 4 wks. At the time of early plantar muscle reinnervation, the plantar muscle CMAPs in the H3-treated group had lower amplitudes (fewer functional motor axons; Figure 2A) and longer latencies (less mature axons; Figure 2B). This H3-induced electrophysiological delay was no longer distinguishable from the following week, presumably because all regenerating axons reached their plantar targets by that time (Figures 2A, B). Furthermore, given the small magnitude of the delay, the SFI recovery remained indistinguishable between H3- and vehicle-treated mice, reaching a plateau at 80% below baseline (Figure 2C), consistent with the poor recovery of CMAP amplitude (Figure 2A). Although the number of tibial nerve myelinated axons was similar in the H3- and vehicle-treated groups (Figure 2D) at the completion of the study (9 wks after the lesion and 5 wks after treatment), the H3-treated axons were smaller (Figure 2E), consistent with the early delay in growth. H3 treatment had no electrophysiological or histological effects on the contralateral (uninjured) nerves (Figures 2A–E).

The delay in regeneration caused by H3 treatment after transection in mice had no functional consequences but was intriguingly opposite to the accelerated recovery after crush in rats. We therefore repeated the mouse experiments using crush injury instead of transection. We found that H3 treatment did not delay the regeneration of tibial nerve myelinated axons after crush (Figures 3A–E). Instead, it accelerated the regeneration, although the effect was smaller than in the rat model and was only noticed as earlier electrophysiological recovery at a time point when CMAPs could be evoked from the H3- but not vehicle-treated tibial nerves (Figures 3A, B).

In previous studies, we proposed that increased branching of axonal sprouts during growth after nerve section and repair could slow regeneration (37,38). Because H3 promoted neurite extension, it was feasible to suggest that in an ideally guided growth environment provided by the crush lesion, H3 accelerated regeneration, whereas after section H3 caused increased branching that slowed regeneration. To address this possibility, we investigated the effect of H3 on neurite branching *in vitro*. As an experimental system, we used primary hippocampal neurons, in which both S100A4 and H3 act as neurite promoters (10,14,16). To mimic the characteristic growth environment in the PNS, the cells were plated on laminin (Figure 4, Ctl). Both H3 and S100A4 induced a robust neurite outgrowth from primary neurons additive to that triggered by the laminin substratum (Figures 4A, B). Moreover, the cells stimulated by S100A4 or H3 displayed more prominent branching compared with those grown in the presence of laminin only. Quantification showed that the average number of neurites originating from the soma ("primary neurites") was significantly higher in the S100A4- and H3-treated cells than in the untreated controls (Figure 4C). Moreover, the H3 peptide, but not S100A4, strongly increased the average number of branching points per neurite length (Figure 4D, branching) and decreased the relative length of the longest neuronal process (Figure 4E, polarity). To confirm these effects in the experimental system relevant to our *in vivo* studies, we performed a

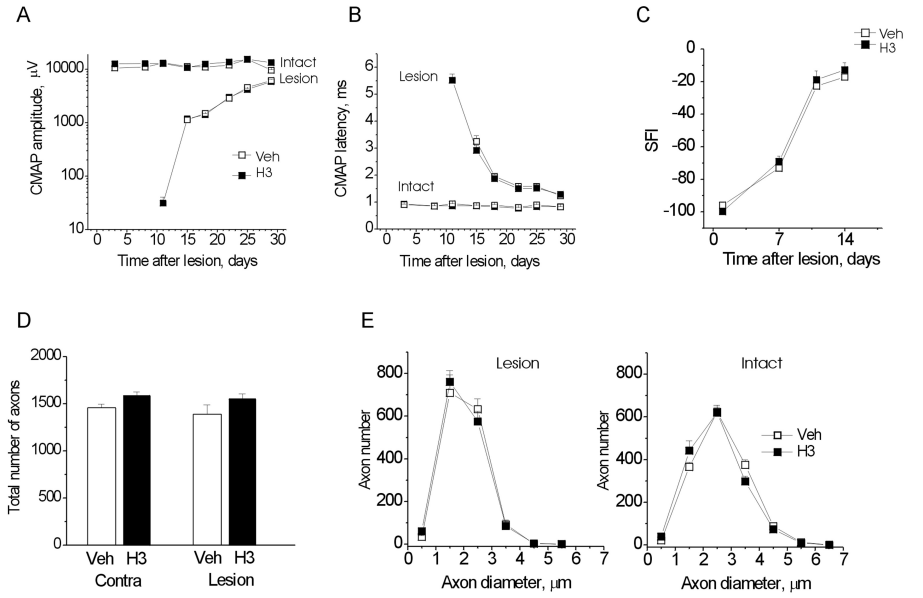

Figure 3. The H3 peptide does not alter axonal regeneration after the nerve crush in mice. (A, B) Development of CMAP amplitude (A) and conduction velocity (B) in unoperated (Intact) and operated (Lesion) nerves in the vehicle (Veh)- and H3-treated animals. (C) Recovery of the functional index (SFI). (D, E) Total number of fibers (D) and myelinated fiber distribution (E) at 4 wks after lesion. (A–C) Number of animals, n = 10/11 (Veh/H3). (D, E) n = 10/10.

similar set of experiments in cultured motor neurons (cell identity verified by the neurofilament-HT staining; Figure 4F; 35). In this experimental setup, H3 also induced profound neurite outgrowth (Figure 4G), increased both primary and secondary neurite branching (Figures 4H, I, respectively) and decreased neuronal polarity (Figure 4J). Altogether, these results show that H3 not only stimulates neurite extension, but also induces "bushy" neurite morphology, a feature that could be responsible for the lesion type–dependent effect of H3 on axonal regeneration.

H3 Peptide Attenuated the Progression of Neuropathy in $P_0^{-/-}$

S100A4 and its mimetics not only promote neuritogenesis, but also act as prosurvival factors in brain injury (10). We therefore investigated the neuroprotective effect of the H3 peptide in a clinically relevant mouse model of a peripheral neurodegeneration, caused by deficiency in the gene for the adhesion molecule P_0. $P_0^{-/-}$ show a severe and progressive dysmyelinating neuropathy from birth, with compromised myelin compaction, hypomyelination and distal axonal degeneration, which in 2-month-old mice leads to markedly abnormal CMAPs with amplitudes reduced by 90%, latencies increased by 300% and rotarod endurance time reduced by 70% compared with wild-type littermates (24). We investigated whether H3 treatment can alter progression of the neuropathy over 1 month. To account for the large variability of neuropathic deterioration, comparisons were performed per nerve (or per animal in the case of rotarod). The measurements after the treatment (post) were normalized to corresponding measurements before treatment, which was set to 100% (Figure 5).

H3 treatment for 1 month had a beneficial effect on P_0 neuropathy. H3 nearly prevented the increase of CMAP latency (reflecting the demyelination of the fastest conducting axon; Figure 5B) and, to a lesser extent, attenuated the decline of CMAP (Figure 5A). The deterioration of motor performance measured by rotarod endurance time also tended to be attenuated in H3-treated mice ($p = 0.12$; Figure 5C). These findings were supported by the histological results. By the end of the observation period, the H3-treated animals had ~30% more myelinated axons than the vehicle group (Figure 5D). This difference was mostly accounted for by the larger number of small fibers (Figure 5E). Although the precise cause of axonal loss secondary to demyelination in $P_0^{-/-}$ mice remains unknown, detailed electrophysiological studies have shown that with progression of neuropathy, the $P_0^{-/-}$ myelin becomes thinner until it disappears completely over extended axonal internodes and that it is these segments from which axons degenerate (39–41). Here, we found that the myelin was thicker in the H3-treated group than in the vehicle-treated group for all axonal diameters (Figure 5F). Furthermore, we detected strong S100A4 immunoreactivity in the sciatic nerves of $P_0^{-/-}$, where it was expressed by Schwann cells and most of the axons (Figure 6), suggesting that intracellular S100A4 could also modulate progression of neuropathy in this experimental model.

DISCUSSION

In this study, we investigated the effect of S100A4 mimetics in the injured PNS, with a focus on the survival and regeneration of myelinated axons. We found that the H3 mimetic peptide changed the time course of peripheral nerve regeneration without affecting the final outcome and had important long-term axonal prosurvival effects in a mouse model of CMT.

Although the S100A4 protein is mainly known as a metastasis promoter, it has recently emerged as an important player in neuroregeneration in the CNS (10). Moreover, similarity exists between the patterns of S100A4 expression in the CNS and PNS, where the protein is detected in astrocytes and Schwann cells, respectively, and is strongly upregulated after injury (9,17,18). Accordingly, here we found that S100A4 was expressed by

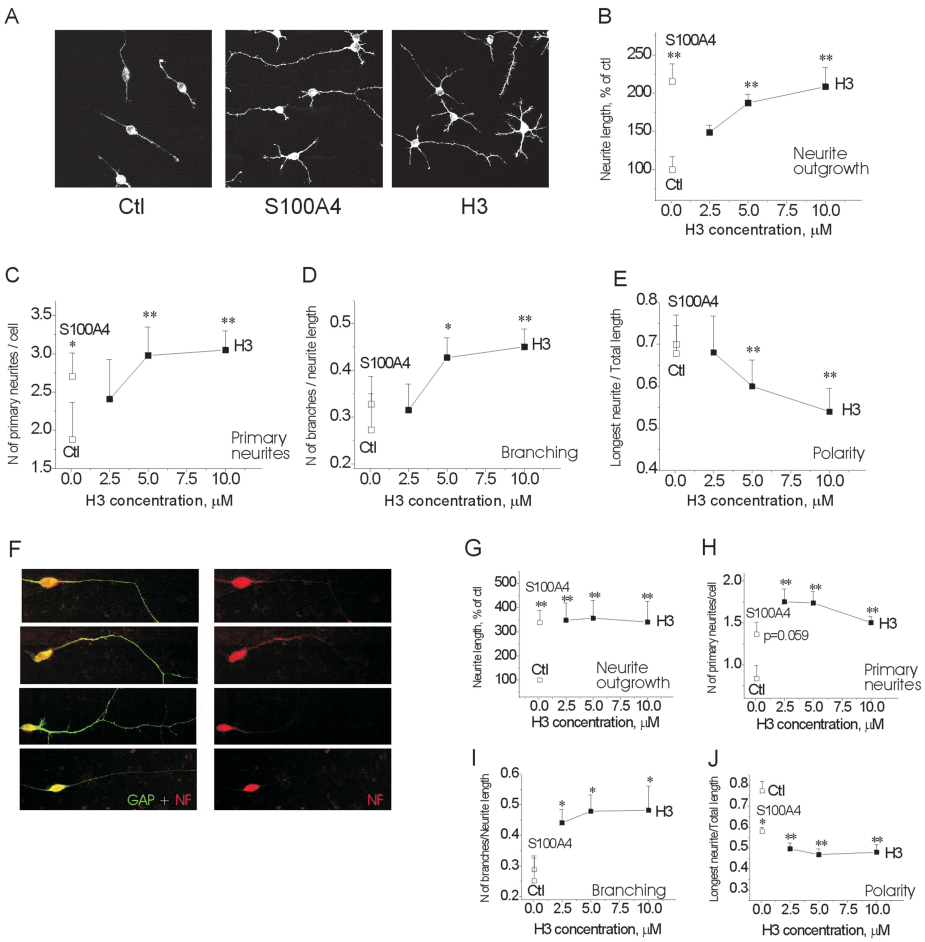

Figure 4. The H3 peptide increases neuronal branching in primary cultures of hippocampal and motor neurons. (A) Representative micrographs of hippocampal neurons grown on the laminin substratum in the absence of soluble ligands (Ctl) or in the presence of S100A4 or H3. (B–E: Hippocampal neurons, field 120 × 120 μm.) Effect of S100A4 (10 μmol/L) and the H3 peptide on average neurite length per cell (B), number of primary neurites per cell (C), number of branching points per neurite length (D) and ratio of longest neurite length to total neurite length per cell (E) are shown. (F–I: motoneurons.) (F) Representative micrographs of motoneurons double stained for GAP-43 and neurofilament-HT (NF), field 100 × 30 μm. (G–J) Effect of S100A4 (10 μmol/L) and the H3 peptide on average neurite length per cell (G), number of primary neurites per cell (H), number of branching points per neurite length (I) and ratio of longest neurite length to total neurite length per cell (J). (B–J) ANOVA versus untreated controls (Ctl); four independent experiments were performed.

Schwann cells and selected axons in the sciatic nerves of both wild-type and $P_0^{-/-}$ mice (Figure 6). Interestingly, this S100A4 expression in the intact mouse PNS was in contrast to the absence of S100A4 in the uninjured mouse brain, where the same antibodies did not detect it (10). This observation suggests that S100A4 may have a role in normal nerve function.

In the injured CNS, S100A4 knockout leads to increased neuronal loss, whereas peptides mimicking functions of S100A4, H3 and H6 have neuroprotective effects (10). Notably, however, a fundamental difference exists in the peptides' origins: H6 is a "unique" motif in the S100A4 sequence with little homology to other S100 proteins, whereas H3 is a "common" motif for many S100 proteins. This fact may explain the different effects of the peptides in the PNS, where H3 accelerated recovery of the entire fiber population after nerve crush, whereas the H6 effects were confined to the sensory fiber subpopulation. Indeed, as a "shared" motif, H3 is more likely to interact with targets common for many S100 proteins, the best characterized of which is the receptor for advanced glycation end products (RAGE [42,43]). By using surface plasmon resonance analysis, we previously observed direct binding of H3 to RAGE (10). Importantly, pharmacological blockade of RAGE or the expression of its signal transduction–deficient version impairs restoration of the motor function after sciatic nerve crush (44), making this receptor a possible mediator of the biological effects of H3 in the peripheral nerve.

In this study, we observed dual effects of H3 on the time course of nerve regeneration. The peptide accelerated recovery after the crush lesion, but transiently delayed regeneration after nerve transection and reconstruction. In previous studies, we proposed that increased branching of axonal sprouts could account for the slower regeneration after transection than after crush nerve injuries (37,38). Here we showed that *in vitro* H3 promotes not only neuritogenesis, but also neurite branching (Figure 4). It is therefore likely that increased axonal branching *in vivo* would slow down regeneration after transection, whereas an opposite effect would be seen in the ideally confined growth environment of the crush lesion, where branching is restricted.

A time window exists within which axons must grow through the distal nerve stump for recovery after nerve lesions to be optimal (45). Nevertheless, despite increased branching, H3 did not detrimentally affect the functional outcome consistent with previous observations that strategies to reduce the excessive sprouting at the lesion site had no major impact on functional recovery (46). It remains to be clarified to which extent the increased branching after H3 would

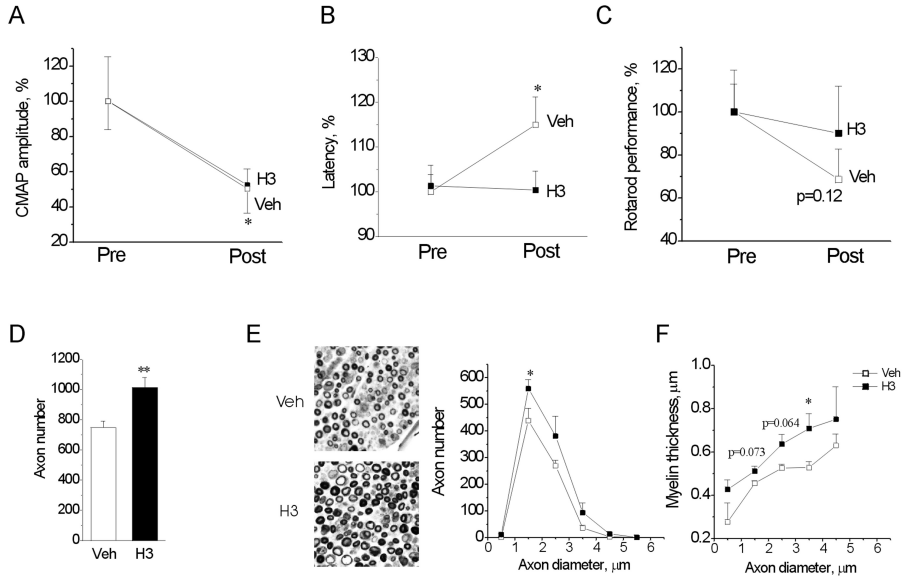

Figure 5. The H3 peptide delays neurodegeneration caused by deficiency in the myelin P_0 gene. (A–C) Development of CMAP amplitude (A), conduction velocity (B) and rotarod performance (C) in $P_0^{-/-}$ mice treated with vehicle (Veh) or the H3 peptide for 30 d. Measurements were performed before treatment (Pre) start and immediately after treatment finish (Post) and were normalized to the Pre value in each group (set to 100%). *$p < 0.05$ versus Pre, two-tailed *t* test. (D–F) Total number of fibers (D), myelinated fiber distribution (E) and myelin thickness distribution (F) at the end of the treatment period. (E, left) Representative images of sciatic nerves from the Veh- and H3-treated animals at the end of the treatment period; 50 × 50 μm fields are shown. *$p < 0.05$ versus Veh, two-tailed *t* test. (A–C) Number of analyzed nerves, n = 13/15 (Veh/H3). (D, E) n = 6/8.

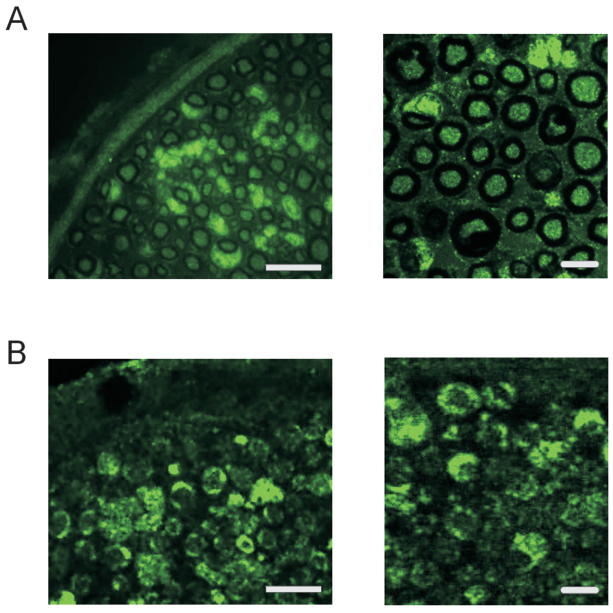

Figure 6. S100A4 is expressed in the mouse PNS. (A, B) Representative fluorescent micrographs of the intact sciatic nerve of wild-type (A) and $P_0^{-/-}$ (B) mice at two magnifications; n = 4 animals/group. Bars, 100 μm (left) and 5 μm.

be beneficial for pathway selection and reinnervation accuracy (47,48). This finding also suggests the intriguing possibility that S100A4, too, may have multiple roles in the lesioned nerve. Indeed, because S100A4 is upregulated immediately proximal to the injury and in the distal stump (18), it is in the position to affect both the axon crossing the lesion site and a subsequent axon regrowth.

An often-neglected aspect of nerve injury is its effect on the neuronal cell survival. Spinal neurons (especially motoneurons) that have their axons injured very close to the cell bodies (proximal lesions) may fail to regenerate their peripheral axon and change polarity by extending dendrite-derived supernumerary axons or even die (49). Nevertheless, some studies indicate that distal axonal injuries may trigger an apoptotic-like degeneration, most notably of small sensory neurons in the dorsal root ganglia, giving rise to permanent deficits (50). Here we found that the effects of H3 treatment after injury were only transient and did not seem to influence the outcome of peripheral nerve regeneration. We therefore did not attempt to analyze in detail to which extent an injury-induced neuronal loss occurred in the motor and sensory axon populations in our models.

In contrast to nerve regeneration models, H3 strongly affected the long-term outcome in a mouse model of a neuropathy caused by deficiency in the P_0 gene. Chronic treatment with the peptide attenuated the deterioration of nerve conduction and postponed demyelination and axonal loss (Figure 5). This result was in agreement with effects of H3 in animal models of brain trauma, where the prosurvival but not neuritogenic activity was crucial for the outcome (10). Interestingly, earlier reports show that Tacrolimus (FK506), an agent with immunomodulatory properties, accelerating peripheral nerve regeneration, aggravated axonopathic features in patients and P_0 mutant mice (51,52). Taken together, these findings suggest that the effects of H3 on P_0-related axonal survival

and sprouting are distinct. Our data provide proof of principle that mimicking the S100A4 activity by H3 administration protects axons from secondary injury in the context of severe demyelination in a P_0 model. Further studies should be carried out to clarify whether this effect is limited to the particular context of the P_0 deficiency, or it can be extended to other demyelinating or axonal forms of CMT (53,54).

At least two mechanisms may underlie the effects of H3 in the PNS. As we have previously shown, H3 (a) exerts direct neurotrophic effect on neurons and (b) increases S100A4 expression in glia of the injured brain. The second mechanism is particularly interesting, given that S100A4 is expressed in Schwann cells and that both peripheral nerve regeneration and presumably axonal degeneration in CMT (24,25) depend on axon–Schwann cell interaction. If S100A4, similar to another neuroactive protein of the family, S100B (55), is released by Schwann cells, it may exert direct axonal effects. Moreover, extra- and intracellular S100A4 may also modulate Schwann cell function to produce additional neurotrophic factors. Such modulation was observed in glia of the lesioned brain, where S100A4 deficiency led to a downregulation of the neuroprotective protein metallothionein I + II (10).

To summarize, our data suggest that S100A4 mimetics are a novel class of molecules capable of modulating the PNS response to injury, especially in the context of demyelinating neuropathies with secondary axonal loss, such as CMT. Moreover, representing biologically active motifs of S100A4, the peptides provide a valuable insight into S100A4 roles in the PNS.

For interpretation of the results of this study, the limitations of the mimetic approach should be considered. First, H3 and H6 are peptide fragments of S100A4 and probably only partially reproduce its function. Second, in our experiments, the peptides were administered systemically and thus only mimicked the extracellular effects of S100A4. However, even with these limitations, the obtained results suggest that S100A4 may be involved in multiple processes in the damaged PNS, affecting axonal growth, branching and survival. Moreover, because H3 represents a homologous motif in S100 proteins, several members of the S100 family may have yet undiscovered roles in PNS pathologies. It is therefore important to further investigate S100 roles in the PNS plasticity by using transgenic animal models. This aspect and the mechanisms underlying the effects of S100 on axonal growth and survival will need to be addressed in future studies.

CONCLUSION

To summarize, our results for the first time suggest a neuroprotective function for S100A4 and its peptide mimetics in the PNS. The peptides derived from the neurotrophic motifs of S100A4 may emerge as novel tools to enhance axonal sprouting and survival, especially in the context of neuropathies with secondary axonal loss, such as CMT. Moreover, our data suggest that other S100 proteins, sharing high homology in these motifs, may have previously unrecognized contributions to PNS pathologies.

ACKNOWLEDGMENTS

The project was supported by the Lundbeck Foundation, Novo Nordisk Foundation, Danish Medical Research Council, Ludvig and Sara Elsass Foundation, Foundation for Research in Neurology and the Jytte and Kaj Dahlboms Foundation. We would like to thank Irina Korshunova for help with genotyping the P_0 mice and Lis Hansen for expert technical assistance with the histological preparations.

DISCLOSURE

The authors declare that they have no competing interests as defined by *Molecular Medicine*, or other interests that might be perceived to influence the results and discussion reported in this paper.

REFERENCES

1. Donato R. (2003) Intracellular and extracellular roles of S100 proteins. *Microsc. Res. Tech.* 60:540–551.
2. Salama I, Malone PS, Mihaimeed F, Jones JL. (2008) A review of the S100 proteins in cancer. *Eur. J. Surg. Oncol.* 34:357–64.
3. Goyette J, Geczy CL. (2011) Inflammation-associated S100 proteins: new mechanisms that regulate function. *Amino Acids*. 41:821–42.
4. Zimmer DB, Chaplin J, Baldwin A, Rast M. (2005) S100-mediated signal transduction in the nervous system and neurological diseases. *Cell Mol. Biol. (Noisy-le-grand).* 51:201–14.
5. Shepherd CE, *et al.* (2006) Inflammatory S100A9 and S100A12 proteins in Alzheimer's disease. *Neurobiol. Aging*. 27:1554–63.
6. Lisachev PD, *et al.* (2010) A comparison of the dynamics of S100B, S100A1, and S100A6 mRNA expression in hippocampal CA1 area of rats during long-term potentiation and after low-frequency stimulation. *Cardiovasc. Psychiatry Neurol*. 2010:720958.
7. Garrett SC, Varney KM, Weber DJ, Bresnick AR. (2006) S100A4, a mediator of metastasis. *J. Biol. Chem.* 281:677–80.
8. Boye K, Maelandsmo GM. (2010) S100A4 and metastasis: a small actor playing many roles. *Am. J. Pathol.* 176:528–35.
9. Kozlova EN, Lukanidin E. (2002) Mts1 protein expression in the central nervous system after injury. *Glia.* 37:337–48.
10. Dmytriyeva O, *et al.* (2012) The metastasis-promoting S100A4 protein confers neuroprotection in brain injury. *Nat. Commun.* 3:1197.
11. Zhang KH, Han S, Lu PH, Xu XM. (2004) Upregulation of S100A4 after spinal cord transection in adult rats. *Acta. Pharmacol. Sin.* 25:1007–12.
12. Stary M, Schneider M, Sheikh SP, Weitzer G. (2006) Parietal endoderm secreted S100A4 promotes early cardiomyogenesis in embryoid bodies. *Biochem. Biophys. Res. Commun*. 343:555–63.
13. Yammani RR, Long D, Loeser RF. (2009) Interleukin-7 stimulates secretion of S100A4 by activating the JAK/STAT signaling pathway in human articular chondrocytes. *Arthritis Rheum.* 60:792–800.
14. Novitskaya V, *et al.* (2000) Oligomeric forms of the metastasis-related Mts1 (S100A4) protein stimulate neuronal differentiation in cultures of rat hippocampal neurons. *J Biol. Chem.* 275:41278–86.
15. Pedersen MV, *et al.* (2004) The Mts1/S100A4 protein is a neuroprotectant. *J. Neurosci. Res.* 77:777–86.
16. Kiryushko D, *et al.* (2006) Molecular mechanisms of Ca(2+) signaling in neurons induced by the S100A4 protein. *Mol. Cell. Biol.* 26:3625–38.
17. Kozlova EN, Lukanidin E. (1999) Metastasis-associated mts1 (S100A4) protein is selectively expressed in white matter astrocytes and is upregulated after peripheral nerve or dorsal root injury. *Glia.* 27:249–58.
18. Sandelin M, Zabihi S, Liu L, Wicher G, Kozlova EN. (2004) Metastasis-associated S100A4 (Mts1) protein is expressed in subpopulations of sensory

and autonomic neurons and in Schwann cells of the adult rat. *J. Comp. Neurol.* 473:233–43.
19. Fang Z, Forslund N, Takenaga K, Lukanidin E, Kozlova EN. (2006) Sensory neurite outgrowth on white matter astrocytes is influenced by intracellular and extracellular S100A4 protein. *J. Neurosci. Res.* 83:619–26.
20. Haglid KG, *et al.* (1997) S-100beta stimulates neurite outgrowth in the rat sciatic nerve grafted with acellular muscle transplants. *Brain Res.* 753:196–201.
21. Wolthers M, Moldovan M, Binderup T, Schmalbruch H, Krarup C. (2005) Comparative electrophysiological, functional, and histological studies of nerve lesions in rats. *Microsurgery.* 25:508–19.
22. Giese KP, Martini R, Lemke G, Soriano P, Schachner M. (1992) Mouse P0 gene disruption leads to hypomyelination, abnormal expression of recognition molecules, and degeneration of myelin and axons. *Cell.* 71:565–76.
23. Martini R, Zielasek J, Toyka KV, Giese KP, Schachner M. (1995) Protein zero (P0)-deficient mice show myelin degeneration in peripheral nerves characteristic of inherited human neuropathies. *Nat. Genet.* 11:281–6.
24. Moldovan M, *et al.* (2011) Na(v)1.8 channelopathy in mutant mice deficient for myelin protein zero is detrimental to motor axons. *Brain.* 134:585–601.
25. Nave KA, Sereda MW, Ehrenreich H. (2007) Mechanisms of disease: inherited demyelinating neuropathies: from basic to clinical research. *Nat. Clin. Pract. Neurol.* 453–64.
26. Schmid CD, *et al.* (2000) Immune deficiency in mouse models for inherited peripheral neuropathies leads to improved myelin maintenance. *J. Neurosci.* 20:729–35.
27. *OECD principles of Good Laboratory Practice: (as revised in 1997).* 1998. Paris: Organisation for Economic Co-operation and Development [OECD], Environment Directorate; [cited 2013 Mar 25]. Available from: OECD Environment Directorate, Environmental Health and Safety Division, Paris, France; http://www.oecd.org/ehs/.
28. European Parliament; Council of the EU. (2010) Directive 2010/63/EU of the European Parliament and of the Council of 22 September 2010 on the protection of animals used for scientific purposes. *Off. J. European Union*. 53:L 276/33–79.
29. Committee for the Update of the Guide for the Care and Use of Laboratory Animals, Institute for Laboratory Animal Research, Division on Earth and Life Studies, National Research Council of the National Academies. (2011) *Guide for the Care and Use of Laboratory Animals.* 8th edition. Washington (DC): National Academies Press; [cited 2013 Mar 25]. Available from: http://www.aaalac.org/resources/theguide.cfm.
30. Moldovan M, Alvarez S, Krarup C. (2009) Motor axon excitability during Wallerian degeneration. *Brain.* 132:511–23.
31. Bain JR, Mackinnon SE, Hunter DA. (1989) Functional evaluation of complete sciatic, peroneal, and posterior tibial nerve lesions in the rat. *Plast. Reconstr. Surg.* 83:129–38.
32. de Medinaceli L, Freed WJ, Wyatt RJ. (1982) An index of the functional condition of rat sciatic nerve based on measurements made from walking tracks. *Exp. Neurol.* 77:634–43.
33. Alagappan D, *et al.* (2009) Brain injury expands the numbers of neural stem cells and progenitors in the SVZ by enhancing their responsiveness to EGF. *ASN Neuro.* 1:e00009.
34. Soroka V, *et al.* (2002) Induction of neuronal differentiation by a peptide corresponding to the homophilic binding site of the second Ig module of the neural cell adhesion molecule. *J. Biol. Chem.* 277:24676–83.
35. Haastert K, *et al.* (2005) Rat embryonic motoneurons in long-term co-culture with Schwann cells: a system to investigate motoneuron diseases on a cellular level in vitro. *J. Neurosci. Methods.* 142:275–84.
36. Pankratova S, *et al.* (2012) A new agonist of the erythropoietin receptor, Epobis, induces neurite outgrowth and promotes neuronal survival. *J. Neurochem.* 121:915–23.
37. Fugleholm K, Schmalbruch H, Krarup C. (1994) Early peripheral nerve regeneration after crushing, sectioning, and freeze studied by implanted electrodes in the cat. *J. Neurosci.* 14:2659–73.
38. Sorensen J, Fugleholm K, Moldovan M, Schmalbruch H, Krarup C. (2001) Axonal elongation through long acellular nerve segments depends on recruitment of phagocytic cells from the near-nerve environment: electrophysiological and morphological studies in the cat. *Brain Res.* 903:185–97.
39. Ey B, Kobsar I, Blazyca H, Kroner A, Martini R. (2007) Visualization of degenerating axons in a dysmyelinating mouse mutant with axonal loss. *Mol. Cell. Neurosci.* 35:153–60.
40. Frei R, *et al.* (1999) Loss of distal axons and sensory Merkel cells and features indicative of muscle denervation in hindlimbs of P0-deficient mice. *J. Neurosci.* 19:6058–67.
41. Samsam M, *et al.* (2003) The Wlds mutation delays robust loss of motor and sensory axons in a genetic model for myelin-related axonopathy. *J. Neurosci.* 23:2833–9.
42. Hofmann MA, *et al.* (1999) RAGE mediates a novel proinflammatory axis: a central cell surface receptor for S100/calgranulin polypeptides. *Cell.* 97:889–901.
43. Huttunen HJ, *et al.* (2000) Coregulation of neurite outgrowth and cell survival by amphoterin and S100 proteins through receptor for advanced glycation end products (RAGE) activation. *J. Biol. Chem.* 275:40096–105.
44. Rong LL, *et al.* (2004) RAGE modulates peripheral nerve regeneration via recruitment of both inflammatory and axonal outgrowth pathways. *FASEB J.* 18:1818–25.
45. Krarup C, Archibald SJ, Madison RD. (2002) Factors that influence peripheral nerve regeneration: an electrophysiological study of the monkey median nerve. *Ann. Neurol.* 51:69–81.
46. Skouras E, Ozsoy U, Sarikcioglu L, Angelov DN. (2011) Intrinsic and therapeutic factors determining the recovery of motor function after peripheral nerve transection. *Ann. Anat.* 193:286–303.
47. Brushart TM. (1988) Preferential reinnervation of motor nerves by regenerating motor axons. *J. Neurosci.* 8:1026–31.
48. Uschold T, Robinson GA, Madison RD. (2007) Motor neuron regeneration accuracy: balancing trophic influences between pathways and end-organs. *Exp. Neurol.* 205:250–6.
49. Meehan CF, MacDermid VE, Montague SJ, Neuber-Hess M, Rose PK. (2011) Dendrite-derived supernumerary axons on adult axotomized motor neurons possess proteins that are essential for the initiation and propagation of action potentials and synaptic vesicle release. *J. Neurosci.* 31:6732–40.
50. Terenghi G, Hart A, Wiberg M. (2011) The nerve injury and the dying neurons: diagnosis and prevention. *J. Hand Surg.* 36:730–4.
51. Weimer LH, Podwall D. (2006) Medication-induced exacerbation of neuropathy in Charcot Marie Tooth disease. *J. Neurol. Sci.* 242:47–54.
52. Ip CW, Kroner A, Kohl B, Wessig C, Martini R. (2009) Tacrolimus (FK506) causes disease aggravation in models for inherited peripheral myelinopathies. *Neurobiol. Dis.* 33:207–12.
53. d'Ydewalle C, Benoy V, Van Den Bosch L. (2012) Charcot-Marie-Tooth disease: emerging mechanisms and therapies. *Int. J. Biochem. Cell. Biol.* 44:1299–304.
54. ten Asbroek AL, *et al.* (2005) Expression profiling of sciatic nerve in a Charcot-Marie-Tooth disease type 1a mouse model. *J. Neurosci. Res.* 79:825–35.
55. Perrone L, Peluso G, Melone MA. (2008) RAGE recycles at the plasma membrane in S100B secretory vesicles and promotes Schwann cells morphological changes. *J. Cell. Physiol.* 217:60–71.